BNL-24914

# RUTHENIUM OXIDE ANODES FOR SOLID POLYMER ELECTROLYTE WATER ELECTROLYZERS: ELECTROCHEMICAL AND ELLIPSOMETRIC STUDIES*

P.W.T. Lu and S. Srinivasan

Department of Energy and Environment
Brookhaven National Laboratory
Upton, New York 11973



## ABSTRACT

Ruthenium oxide ($RuO_x$) is of considerable interest for the development of solid polymer electrolyte (SPE) water electrolyzers because of its high catalytic activity for the oxygen evolution reaction. As a first approach toward the understanding of the kinetics of this reation, ellipsometric investigation of oxide films on Ru anodes was carried out in a 25% trifluoromethane sulfonic acid. The formation of $Ru(OH)_3$ film commences at $\sim$ 0.73 V. At potentials above 0.94 V, $Ru(OH)_3$ is further oxidized to $RuO_2 \cdot YH_2O$ film. In situ optical analysis of Ru electrodes confirms that oxide films formed anodically can be removed by electroreduction. The critical potential at which Ru corrodes rapidly to $H_2RuO_5$ is $\sim$ 1.45 V. A dissolution-precipitation mechanism is proposed to explain the observed performance degradation with time during oxygen evolution on $RuO_x$ anodes.

## INTRODUCTION

In the General Electric solid polymer (Nafion) electrolyte water electrolyzers, a proprietary Ir-based mixed oxide is normally used as the electrocatalyst for the oxygen evolution reaction (OER). This catalyst exhibits a relatively high oxygen overpotential, which is about 380 mV at a current density of 2 A/cm$^2$ and at 80$^\circ$C (1). Further, it will be most uneconomical to use iridium in large scale electrolyzers. With a view of improving the energy efficiency and minimizing capital cost of solid polymer electrolyte (SPE) water electrolysis cells, investigation and development of highly active and less expensive catalysts to substitute Ir-based mixed oxides as oxygen electrodes are needed.

*This work was performed under the auspices of the U.S. Department of Energy.

## DISCLAIMER

Of the noble metals, ruthenium is most active for the OER in acidic media (2,3). The kinetics of the OER has been extensively investigated on support $RuO_x$ electrodes (4), on crystallites of $RuO_2$ (5) and on Ru (6). It was proposed (6) that, under the Langmuir conditions of intermediate adsorption, the mechanism of the OER on Ru electrodes is

$$S + H_2O \rightleftarrows S\text{-}OH + H^+ + e^- \quad (1)$$

$$2\ S\text{-}OH \rightarrow S\text{-}O + S + H_2O \quad (2)$$

$$2\ S\text{-}O \rightleftarrows 2S + O_2 \quad (3)$$

where S represents an active site on which the OER takes place.

The high catalytic activity of Ru for the OER is marred by its rapid corrosion at highly anodic potentials (2,7). The anodic corrosion of Ru (or more specifically $RuO_x$) has been investigated by use of of charging curves (2,7), a radiochemical technique (8), cyclic voltammetry (9) and atomic absorption spectroscopy (6). It is generally accepted (6,10,11) that, in acidic and neutral solutions, the corrosion of Ru may lead to the formation of a soluble species, $H_2RuO_5$.

More recently, it has been identified (12) that $RuO_x$, prepared by the thermal decomposition of $RuCl_3$, is more active than Ir-based mixed oxides for the OER in SPE cells. At a current density of 1 $A/cm^2$, for example, $RuO_x$ exhibits an oxygen overpotential of ~100 mV less than that on Ir-based mixed oxides. Although the thermally decomposed $RuO_x$ has higher corrosion resistance than the anodized ruthenium oxide (4), the performance for oxygen evolution on this catalyst turns out to decay significantly with time. As a first approach toward the understanding of the mechanism of performance degradation, the nature of oxide films formed on Ru anodes was investigated using ellipsometry. In situ optical analysis of oxide films was conducted in 25% trifluoromethane sulfonic acid, an electrolyte of approximately the same composition as in the Nafion membrane. Further, it has been pointed out that pretreatment on Pt (13) and Ir (14) electrodes using electrochemical techniques results in a significant enhancement in the electrocatalytic activities for the OER. In the present work, effects of preanodization on the kinetic parameters for this reaction were also studied.

## EXPERIMENTAL

### Electrodes and Electrolyte

A ruthenium rod of purity 99.999%, prepared using the zone refining method, was supplied by Inorganic/Organic Research Inc. The working

electrode was fabricated by pressing a Ru rod of ∿1 cm length into a Teflon holder so that only a single face of ∿0.25 $cm^2$ in geometric area was exposed to the electrolyte. This electrode was then mechanically polished as described elsewhere (15) until a mirror-like face was attained. Each freshly polished electrode was cleaned with dilute HCl solution and finally rinsed with triply distilled water.

The 25% trifluoromethane sulfonic acid (TFMSA) solution was prepared from the monohydrate specimen (3M Company) and triply distilled water. In general, a freshly prepared solution had a pale straw color, which gradually became clear after leaving it overnight. A precipitate (black) was found in the container. The measuring solution was purified by anodic pre-electrolysis at a current density of 1 $mA/cm^2$ for ∿48 hours. A reversible hydrogen electrode (RHE) in the same solution (i.e., 25% TFMSA) was employed as the reference electrode. The counter electrode was made of platinum gauze.

## Electrochemical Measurements

A Teflon-sleeved cell, which has been described in detail in the previous work on Ni (16), was used to carry out the combined electrochemical-ellipsometric study of oxide films on Ru anodes. Electrochemical measurements were conducted at 23°C by use of a PAR model 173 potentiostat coupled with a PAR model 175 programmer and a PAR model 376 "log converter."

Tafel relations for oxygen evolution on Ru electrodes were determined using slow (0.1 mV/sec) potentiodynamic techniques. Cyclic voltammetric study on the working electrode was carried out at 10 mV/sec. Prior to each run, the measuring solution in the cell was deaerated with purified $N_2$. The dissolution rate of Ru anodes at constant potentials in the range of 0.9-1.46 V was determined using atomic absorption spectroscopy. An interruptor method was used to measure the ohmic overpotentials (i.e., IR drops) between the working electrode and the reference electrode (17).

## Ellipsometric Measurements

An automatic ellipsometer (Rudolph Research Model RR2000) was employed to conduct <u>in situ</u> optical analysis of oxide films. In order to remove the oxide films formed during the polishing process, each freshly prepared electrode was pretreated at -0.1 V vs. RHE for ∿20 minutes. Ellipsometric and reflectometric data were measured at an angle of incidence 65°, using a monochromatic light of wavelength 5461 Å. The optical readings taken at 0.1 V serve as a reference state. Prior to the measurement of each set of ellipsometric and reflectometric parameters, a stream of purified $N_2$ was passed through the surface of working electrode to eliminate adhering gas bubbles.

## RESULTS AND DISCUSSIONS

### Formation and Transformation of Oxide Films on Ru Electrodes

The variations of ellipsometric and reflectometric parameters [i.e., $\delta\Delta$, $\delta\psi$ and $(\delta R/R)_p$], with respect to the optical readings at 0.1 V, are shown as a function of the polarization potential in Figure 1. Starting at 0.4 V, the electrode potential was increased step-wise to 1.4 V. By holding the electrode at each potential until a stable current was obtained, the ellipsometric and reflectometric parameters were recorded. As illustrated in Figure 1, four distinct regions are well defined in each of the plots of $\delta\Delta$, $\delta\psi$ or $(\delta R/R)_p$ vs. the electrode potential. Three break points are observed approximately at 0.7, 0.9 and 1.1 V.

According to thermodynamic data (18), the reversible potential corresponding to the $Ru/Ru(OH)_3$ couple, that is,

$$Ru + 3H_2O \rightleftarrows Ru(OH)_3 + 3H^+ + 3e^- \qquad (4)$$

is 0.738 V. Further oxidation of $Ru(OH)_3$ film to $RuO_2$, that is,

$$Ru(OH)_3 \rightleftarrows RuO_2 + H_2O + H^+ + e^- \qquad (5)$$

commences at 0.937 V. Since oxide films formed are probably hydrated, the reversible potentials for the $Ru/Ru^{3+}$ and $Ru^{3+}/Ru^{4+}$ couples may be slightly different from the thermodynamic values. Therefore, regions II and III in Figure 1 can be attributed to the formation of $Ru(OH)_3$ film and the conversion of $Ru(OH)_3$ to $RuO_2 \cdot YH_2O$ film occurs probably at $\sim$ 1.1 V. The continuous growth of $RuO_2 \cdot YH_2O$ at potentials above 1.1 V (i.e., region IV in Figure 1) exhibits a different pattern in the variations of ellipsometric and reflectometric parameters.

### Voltammetric Study on Ru Electrode

Figure 2 shows cyclic voltammograms on Ru electrode in a $N_2$-saturated 25% TFMSA. These potentiodynamic i-V profiles are slightly different from those in sulfuric acid (9 19), where broad peaks are usually observed in the potential range of 1.0-1.2 V. The oxide film, formed in the anodic sweep up to 1.2 V, is reduced at $\sim$0.3 V. The higher oxide (possibly, the hydrated $RuO_2$), produced in the potential range of 1.2-1.4 V, is reducible only at potentials below 0.2 V. In a separate cyclic voltammetric study at a slower sweep rate of 1 mV/sec, it was found that the onset potential for oxygen evolution on Ru

electrode is ∿1.35 V in TFMSA. In $HClO_4$ solution, Galizzioli et al. (4) have noted that the OER on $RuO_2$ film starts at ∿1.35 V.

## Electroreduction of Oxide Films

Regarding the reduction of anodic oxide films on Ru electrode, there is a serious discrepancy in the literature. According to the work by Hadzi-Jordanov et al.(19), the surface oxide films on Ru are removable by maintaining the potential in the range of 0.0-0.1 V. Burke and Mulcahy have reported (20) that anodic films on Ru may be reduced by holding the electrode at potentials below 0.2 V. Furthermore, Kinoshita and Ross have noted (21) that $RuO_x$ films, formed in an anodic potential sweep can be reduced in the subsequent cathodic sweep to 0.0 V. On the other hand, Rand, Woods, and Michell have pointed out (9) that anodic oxide films on cycled Ru electrodes cannot be reduced by potential cycling. All these conclusions are drawn simply from cyclic voltammetric studies (9,19-21). In the present work, ellipsometry is used to monitor the surface oxide films in both anodic and cathodic potential sweeps.

The variation of ellipsometric parameters during a complete cycle of potential sweep is shown in Figure 3. In the anodic sweep, the formation of oxide films commences at ∿0.70 V, where both $\Delta$ and $\psi$ start to deviate from the reference state. At the upper limiting potential 1.3 V, significant changes in $\Delta$ and $\psi$ (approximately $-1.0^{\circ}$ and $-0.2^{\circ}$, respectively) were observed, indicating the presence of thick film on the electrode surface. In the cathodic sweep, the electroreduction of oxide film commences at ∿0.8 V. At the end of the cathodic sweep (i.e., at 0.0 V), the variations in $\Delta$ and $\psi$ were approximately zero, which means that the oxide film was completely removed. This result confirms that $RuO_x$ film produced by an anodic sweep can be reduced in the subsequent cathodic sweep (21).

The ellipsometric data, measured under steady-state potentiostatic conditions, are shown in Figure 4. At potentials below 0.937 V (i.e., the reversible potential for the $Ru^{3+}/Ru^{4+}$ couple), the surface film formed on Ru is substantially composed of $Ru(OH)_3$. Thus, if the upper limiting potential is 0.92 V, the electroreduction of this film commences at ∿0.6 V (see Figure 4). This $Ru(OH)_3$ film is completely removed at ∿0.3 V.

As the anodization potential is increased to 1.3 V, the surface film formed on Ru is further oxidized to $RuO_2 \cdot YH_2O$. The electroreduction of $RuO_2 \cdot YH_2O$ film takes place only at potentials below 0.4 V. As demonstrated in Figure 4, this oxide film is essentially removed by holding the electrode at 0.0 V for a long period of time (e.g., 2 hours). Therefore, ellipsometric data confirms that oxide films formed anodically on Ru electrodes can be removed by electroreduction.

## Corrosion of Ru Anode

The degradation of catalytic activity is the most difficult problem in the development of $RuO_x$ for use as an oxygen electrode in SPE water electrolyzers (12). The time dependence of current density for oxygen evolution at constant potentials is illustrated in Figure 5. At first, a freshly prepared Ru electrode was polarized potentiostatically at 1.44 V. The current density decayed significantly in the first few hours, and then reached a stable value in ∿10 hours. This stable current density is only 1/10 of the initial current density on Ru electrode.

After 20 hours of polarization at 1.44 V, the electrode potential was stepped up instantly to 1.46 V. As shown in Figure 5, the current density for the OER increased significantly from ∿0.17 $mA/cm^2$ to ∿10 $mA/cm^2$ in ∿10 hours. By holding the electrode at 1.46 V for 20 hours, the electrolyte which was initially colorless transformed into a golden yellow color. From the atomic absorption spectroscopic analysis, it was found that the average rate of Ru dissolution at this potential was about $1.9 \times 10^{-7}$ $mole/cm^2/hr$.

As demonstrated in Figure 5, the current density for oxygen evolution decayed with time when the electrode potential was lowered to 1.44 V. The final stable current density was about 16 times of the previous value at the same potential. The significant enhancement of current density is possibly due to (i) the surface roughening arising from the Ru dissolution at 1.46 V, or (ii) the presence of Ru-containing species in the electrolyte, which may activate the OER (22,23).

By maintaining the same cell configuration and replacing the electrolyte, the electrode was polarized again at 1.44 V. The dashed line in Figure 5 represents the variation of current density with time in the fresh electrolyte. The final current density was still more than 20 times of the previous value. Therefore, the significant enhancement in current density is essentially due to the anodic dissolution of Ru electrode. The critical potential at which Ru corrodes vigorously is ∿1.45 V. Similarly ellipsometric study on Ir electrode has revealed (14) that Ir oxide films formed by potential cycling corrode significantly at potentials above 1.56 V.

## Effect of Preanodization on the OER

The influence of preanodization on the kinetic parameters for oxygen evolution is shown in Figure 6. Tafel plots were obtained by slow potentiodynamic techniques at a sweep rate of 0.1 mV/sec. Curve 1 represents the Tafel plot for oxygen evolution on an untreated Ru electrode.

After polarizing at 1.44 V for 2 hours, the Tafel plot for the OER corresponds to a slightly lower exchange current density than on the untreated electrode ($1.6 \times 10^{-9}$ and $4.5 \times 10^{-9}$ A/cm$^2$, respectively). Conversely, preanodization at 1.49 V causes Ru dissolution and consequently, a parallel shift of Tafel plot to a higher current density region.

Despite the pretreatment, all the electrodes exhibit Tafel slopes of ∿30 mV/decade. This value (equivalent to ∿RT/2F) strongly supports that the chemical reaction following the discharge step, that is,

$$2\ \text{S-OH} \rightarrow \text{S-O} + \text{S} + \text{H}_2\text{O} \qquad (2)$$

is the rate determining for the OER on Ru electrode (6).

Mechanism of Performance Degradation

The investigation of the mechanism of performance degradation for oxygen evolution on $RuO_x$ catalyst is underway. Preliminary data from ellipsometric study revealed that the current density for the OER decreases exponentially with increasing thickness of $RuO_2$ film. Similar results were observed on Pt electrodes (24). Thus, the growth of $RuO_2$ film seems to inhibit the OER.

In experimental SPE water electrolyzers, $RuO_x$ catalyst mixed with Teflon binder is generally pressed on the face of Nafion membrane. Prior to the electrolysis, no inclusion was present in the membrane as indicated by the electron spectroscopic study of the membrane/electrode assembly (25). It was also found (25) that, after the electrolysis, the average size of $RuO_x$ particles increased and Ru-containing particles were present in the membrane. Thus, it is assumed that, during the electrolysis, small $RuO_x$ particles with higher surface energy corrode to form the soluble species $H_2RuO_5$ (see Figure 7). The species $H_2RuO_5$ is not chemically stable and decomposes, according to the following reaction :

$$H_2RuO_5 + (Y - 1)H_2O \rightarrow RuO_2 \cdot YH_2O + O_2 \qquad (6)$$

to produce stable $RuO_2$ films coated on the surfaces of $RuO_x$ particles. Therefore, the performance degradation for oxygen evolution on $RuO_x$ catalyst is presumably due to the gradual accumulation of $RuO_2 \cdot YH_2O$ on the surface of $RuO_x$ particles by a dissolution-precipitation process as shown in Figure 7. Efforts are being made to obtain evidence to support the dissolution-precipitation model and to develop methods to stabilize $RuO_x$ catalyst.

## CONCLUSIONS

1. Optical analysis of Ru anodes revealed that the formation of $Ru(OH)_3$ film commences at ~0.73 V. The $Ru(OH)_3$ film is further oxidized to $RuO_2 \cdot YH_2O$ at potential above 0.94 V.

2. From the ellipsometric investigation of Ru electrode, it is confirmed that oxide films formed anodically can be removed by electroreduction.

3. The critical potential at which Ru corrodes rapidly in TFMSA is about 1.45 V.

4. The performance degradation for oxygen evolution on $RuO_x$ catalyst is presumably due to the gradual accumulation of $RuO_2$ film on the surface of $RuO_x$ particles by a dissolution-precipitation process.

## ACKNOWLEDGEMENTS

The authors wish to thank Drs. W.E. O'Grady of BNL and S. Gottesfeld of Tel Aviv University for helpful discussions and suggestions.

## REFERENCES

1. A.P. Fickett and F.R. Kalhammer in "Hydrogen; Its Technology and Implications," K.E. Cox and K.D. Williamson, Eds., Vol. 1, Chap. 1, CRC Press, Cleveland (1977).

2. J. Llopis and M. Vazquez, Electrochem. Acta, 11, 633 (1966).

3. L.D. Burke and T.O. O'Meara, J. Chem. Soc., Faraday Trans. I, 68, 839 (1972).

4. D. Galizzioli, F. Tantardini and S. Trasatti, J. Appl. Electrochem. 4, 57 (1974).

5. J. Horkans and M.W. Schafer, J. Electrochem. Soc., 124, 1202 (1977).

6. C. Iwakura, K. Hirao and H. Tamura, Electrochim. Acta, 22, 329 (1977).

7. J. Llopis, I.M. Tordesillas and J.M. Alfayate, Electrochim. Acta, 11, 623 (1966).

8. J. Llopis, J.M. Gamboa and J.M. Alfayate, Electrochim. Acta, 12, 57 (1967).

9. D.A.J. Rand, R. Woods and P. Michell in "Proceedings of the Symposium on Electrode Materials and Processes for Energy Conversion and Storage," J.D.E. McIntyre, S. Srinivasan and F.G. Will, Eds., The Electrochemical Society, 217-233 (1977).

10. T.N. Stoyanovskaya, G.P. Khomchenko and G.D. Vorchenko, Vstn. Mosk. Univ. II Khim., 18, 20 (1963).

11. G.P. Khomchenko, T.N. Stoyanovskaya and G.D. Vorchenko, Zh. fiz. Khim., 38, 434 (1964).

12. A.B. LaConti, private communication.

13. S. Gottesfeld and S. Srinivasan, Extended Abstracts No. 369, 149th Meeting of the Electrochemical Society, Washington, D.C., May 2-7, 1976.

14. S. Gottesfeld and S. Srinivasan, J. Electroanal. Chem., 86, 89 (1978).

15. M.H. Miles, G. Kissel, P.W.T. Lu and S. Srinivasan, J. Electrochem. Soc., 123, 332 (1976).

16. P.W.T. Lu and S. Srinivasan, J. Electrochem. Soc., in press.

17. K.R. Williams, "Introduction to Fuel Cells," pp. 57-63, Elsevier, New York (1966).

18. J. Llopis and I.M. Tordesillas in "Encyclopedia of Electrochemistry of the Elements," A.J. Bard, Ed., Vol. 6, 277, Marcel Dekker, New York (1976).

19. S. Hadzi-Jordanov, H. Angerstein-Kozlowska and B.E. Conway, J. Electroanal. Chem., 60, 359 (1975).

20. L.D. Burke and J.K. Mulcahy, J. Electroanal. Chem., 73, 207 (1976).

21. K. Kinoshita and P.N. Ross, J. Electroanal. Chem., 78, 313 (1977).

22. L.D. Burke and T.O. O'Meara, J. Electroanal. Chem., 36, App. 25 (1972).

23. D.N. Buckley and L.D. Burke, J. Electroanal. Chem., 52, 433 (1974).

24. A. Damjanovic, A.T. Ward and M. O'jea, J. Electrochem. Soc., 121, 1186 (1974).

25. J.L. Weininger and R.R. Russell, J. Electrochem. Soc., in press.

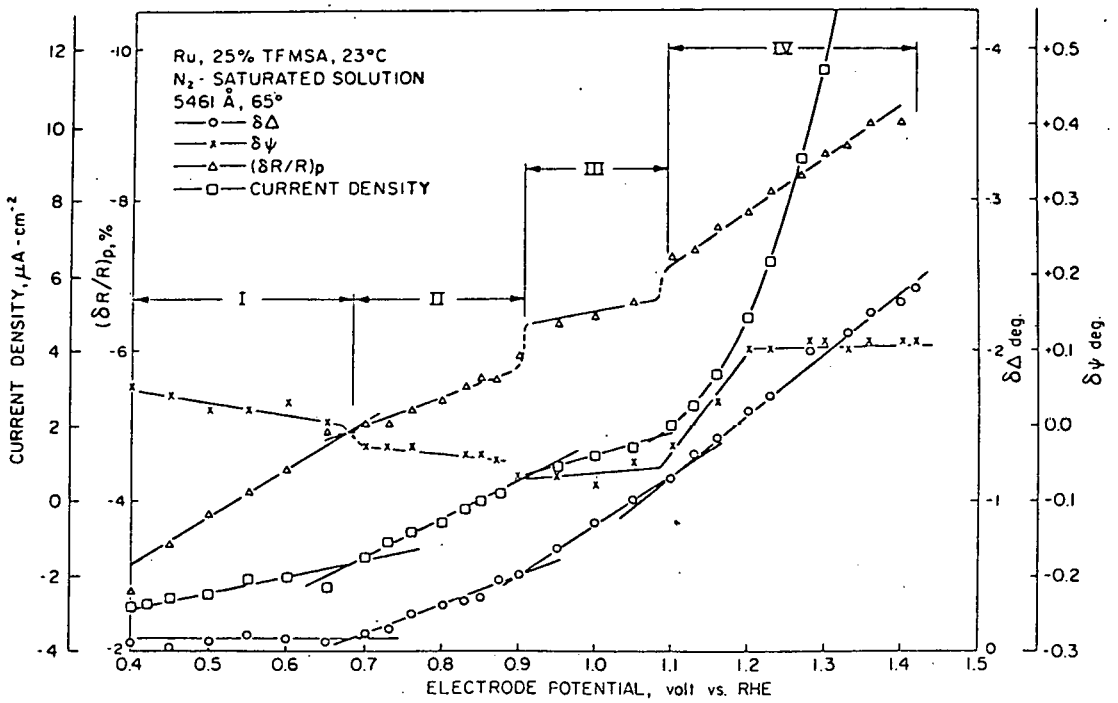


Figure 1. Variations of ellipsometric and reflectometric parameters [i.e., $\delta\Delta$, $\delta\psi$ and $(\delta R/R)_p$] as a function of the electrode potential.

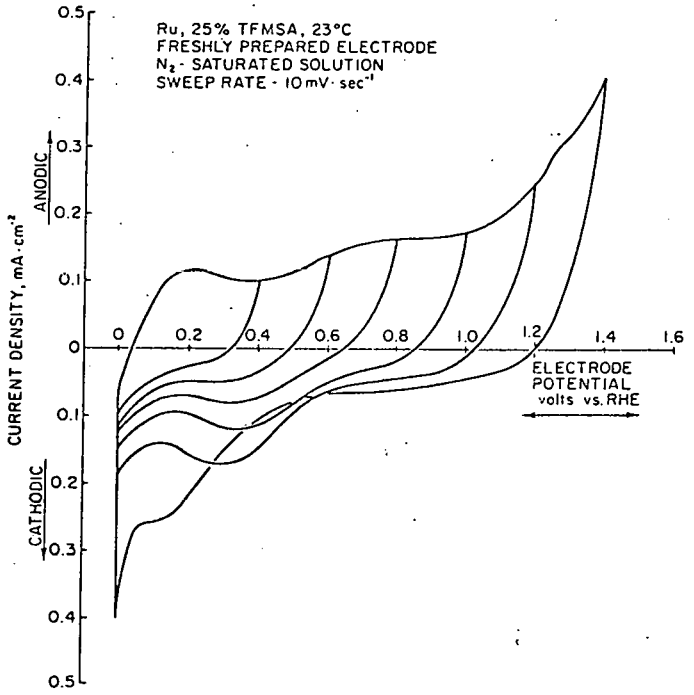


Figure 2. Cyclic voltammograms on Ru electrode at a sweep rate of 10 mV/sec.

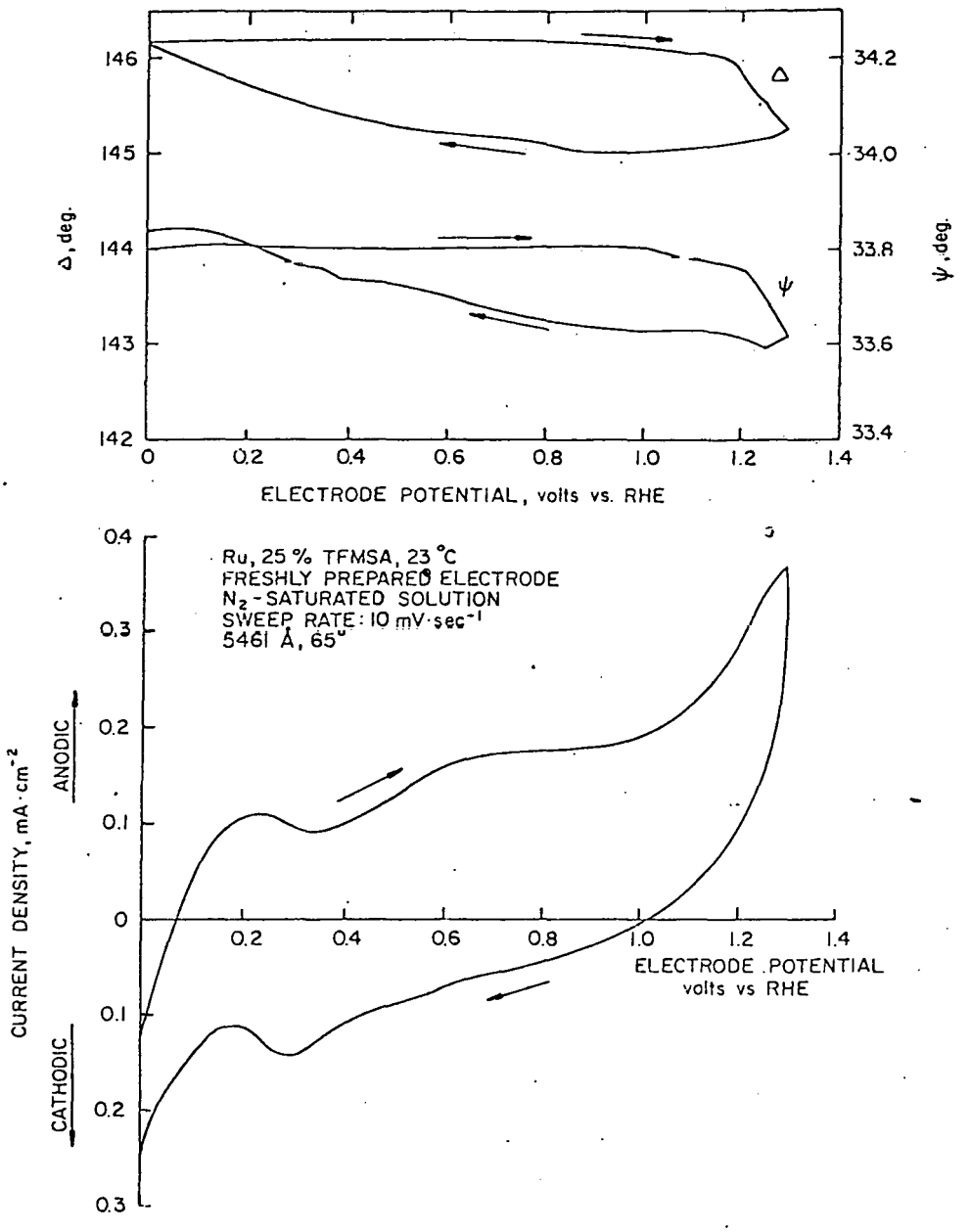


Figure 3. The variation of ellipsometric parameters during a complete cycle of potential sweep.

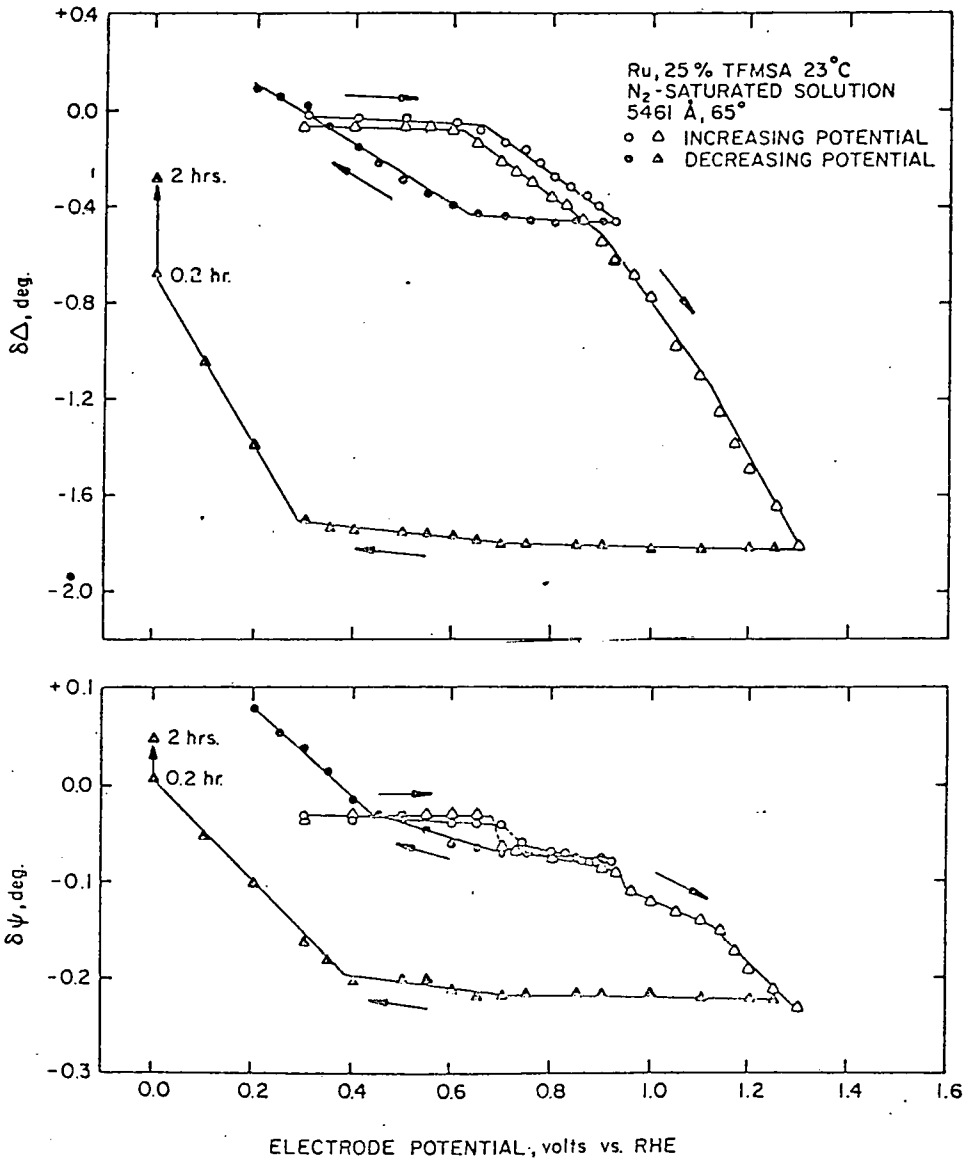


Figure 4. The variation of ellipsometric data, measured under a steady-state potentiostatic condition.

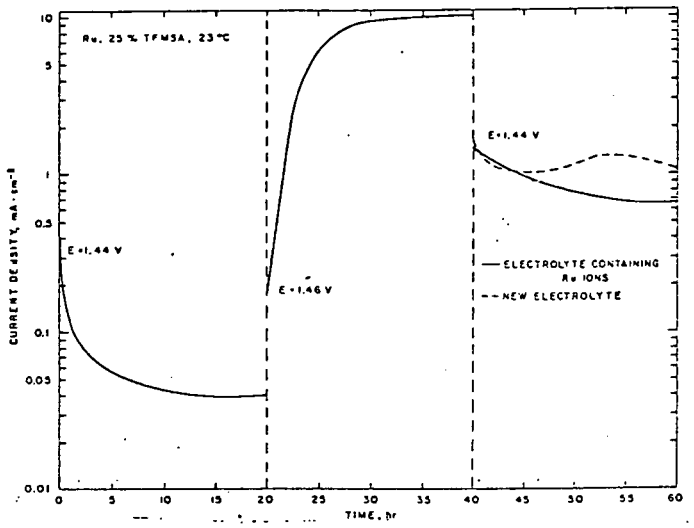


Figure 5. Time dependence of current density for oxygen evolution at constant potentials 1.44 and 1.46 V.

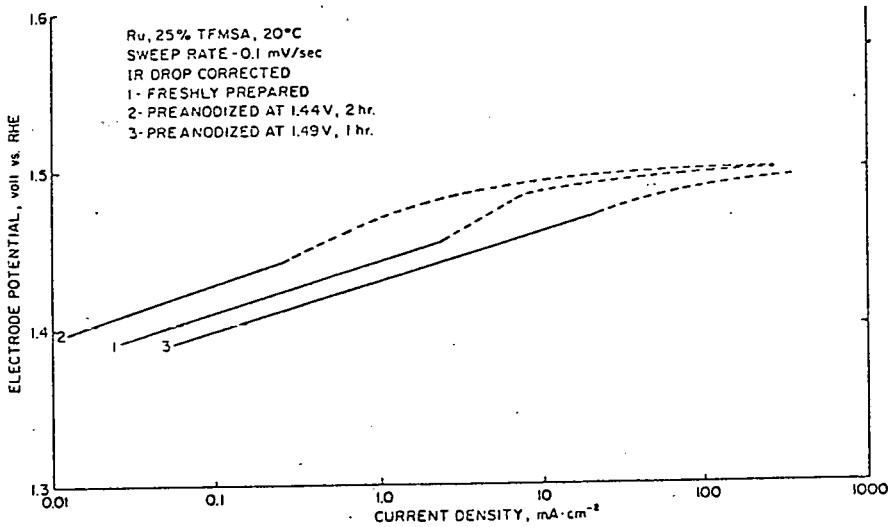


Figure 6. Effects of preanodization on the Tafel plots for oxygen evolution.

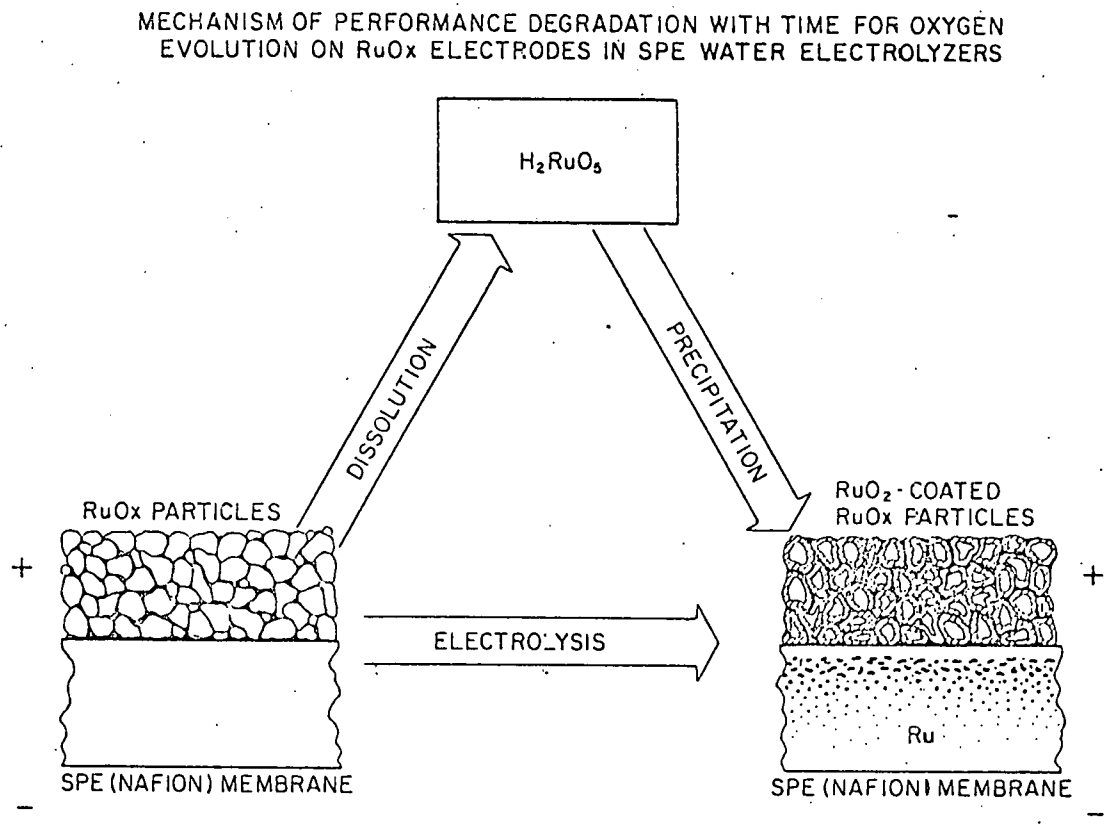


Figure 7. Proposed mechanism of performance degradation with time for oxygen evolution on $RuO_x$ electrodes in SPE water electrolyzers.